AFML-TR-79-4048

(2) LEVEL II

AD A076370

AN ANALYSIS OF RESIDUAL STRESSES AND DISPLACEMENTS DUE TO RADIAL EXPANSION OF FASTENER HOLES

Metals Behavior Branch
Metals and Ceramics Division

July 1979

TECHNICAL REPORT AFML-TR-79-4048

Final Report for Period January 1975 to December 1978

Approved for public release; distribution unlimited

AIR FORCE MATERIALS LABORATORY
AIR FORCE WRIGHT AERONAUTICAL LABORATORIES
AIR FORCE SYSTEMS COMMAND
WRIGHT-PATTERSON AIR FORCE BASE, OHIO 45433

NOTICE

When Government drawings, specifications, or other data are used for any purpose other than in connection with a definitely related Government procurement operation, the United States Government thereby incurs no responsibility nor any obligation whatsoever; and the fact that the government may have formulated, furnished, or in any way supplied the said drawings, specifications, or other data, is not to be regarded by implication or otherwise as in any manner licensing the holder or any other person or corporation, or conveying any rights or permission to manufacture, use, or sell any patented invention that may in any way be related thereto.

This report has been reviewed by the Information Office (OI) and is releasable to the National Technical Information Service (NTIS). At NTIS, it will be available to the general public, including foreign nations.

This technical report has been reviewed and is approved for publication.

Allen F. Grandt Jr.

A. F. GRANDT, Jr., Project Engineer

N G Tupper

NATHAN G. TUPPER, Chief
Metals Behavior Branch
Metals and Ceramics Division

"If your address has changed, if you wish to be removed from our mailing list, or if the addressee is no longer employed by your organization please notify AFML/LLN ,*W-PAFB, OH 45433 to help us maintain a current mailing list".*

Copies of this report should not be returned unless return is required by security considerations, contractual obligations, or notice on a specific document.

AIR FORCE/56780/28 September 1979 — 100

UNCLASSIFIED

SECURITY CLASSIFICATION OF THIS PAGE (When Data Entered)

REPORT DOCUMENTATION PAGE	READ INSTRUCTIONS BEFORE COMPLETING FORM
1. REPORT NUMBER: AFML-TR-79-4048	2. GOVT ACCESSION NO. / 3. RECIPIENT'S CATALOG NUMBER
4. TITLE (and Subtitle): AN ANALYSIS OF RESIDUAL STRESSES AND DISPLACEMENTS DUE TO RADIAL EXPANSION OF FASTENER HOLES	5. TYPE OF REPORT & PERIOD COVERED: Final Report, Jan [redacted] 75-Dec [redacted] 78 / 6. PERFORMING ORG. REPORT NUMBER
7. AUTHOR(s): A. F. Grandt, Air Force Materials Laboratory; R. M. Potter, Air Force Institute of Technology	8. CONTRACT OR GRANT NUMBER(s): 12, 37
9. PERFORMING ORGANIZATION NAME AND ADDRESS: Air Force Materials Laboratory (LLN), Air Force Systems Command, Wright-Patterson AFB, Ohio 45433	10. PROGRAM ELEMENT, PROJECT, TASK AREA & WORK UNIT NUMBERS: 2307, 2307P1, 2307P1 [redacted]
11. CONTROLLING OFFICE NAME AND ADDRESS: Air Force Materials Laboratory, Air Force Wright Aeronautical Laboratories, Air Force Systems Command, Wright-Patterson Air Force Base, Ohio 45433	12. REPORT DATE: Jul [redacted] 79 / 13. NUMBER OF PAGES
14. MONITORING AGENCY NAME & ADDRESS (if different from Controlling Office)	15. SECURITY CLASS. (of this report): UNCLASSIFIED / 15a. DECLASSIFICATION/DOWNGRADING SCHEDULE

16. DISTRIBUTION STATEMENT (of this Report)

Approved for public release; distribution unlimited.

17. DISTRIBUTION STATEMENT (of the abstract entered in Block 20, if different from Report)

18. SUPPLEMENTARY NOTES

19. KEY WORDS (Continue on reverse side if necessary and identify by block number)

Plasticity
Coldworked Holes
Stress Analysis
Mechanical Fasteners

20. ABSTRACT (Continue on reverse side if necessary and identify by block number)

Pre-expanding fastener holes with an oversize mandrel has received considerable attention for use in aircraft structures, since this process has been shown to greatly improve the fatigue life of fastener holes. The deformation theory of plasticity is used here to determine the residual stress and displacement field caused by this process. Employing plane stress assumptions, general results are obtained for various interference levels and are presented in a graphical form useful to the designer. In addition, this analysis indicates → next page

DD FORM 1 JAN 73 1473 EDITION OF 1 NOV 65 IS OBSOLETE

UNCLASSIFIED

SECURITY CLASSIFICATION OF THIS PAGE (When Data Entered)

012 320

Block 20 (cont.)

cont'd

that there is an optimum level of interference dependent primarily on the plate geometry. The optimum interference levels agree well with experience values established by fatigue testing in aircraft structural alloys.

FOREWORD

The research reported herein was accomplished while R. M. Potter was assigned to the Aerospace Research Laboratories (ARL, since disestablished) and subsequently Air Force Institute of Technology, Wright-Patterson Air Force Base, Ohio. Major Potter is presently assigned to 6585 Test Group, Holloman AFB, New Mexico, 88330. Much of the mathematical formulation was accomplished by Prof. T.W. Ting of the University of Illinois while working as a visiting scientist at the Applied Mathematics Laboratory of the Aerospace Research Laboratories, Wright-Patterson Air Force Base, Ohio. A. F. Grandt was the Project Engineer for the Air Force Materials Laboratory. The report covers research conducted under Project No. 2307, Task No. 2307P1, Work Unit No. 2307P102. This report covers work conducted from January 1975 through December 1978.

TABLE OF CONTENTS

LIST OF ILLUSTRATIONS

SECTION I

INTRODUCTION

Since mechanically fastened joints represent one of the most common failure sources in aircraft structures (Reference 1), considerable research has been directed toward developing fatigue resistent fastening systems. One common method to extend the fatigue life is to introduce a controlled residual stress field around the fastener hole by means of an interference fit fastener (Reference 2) or by pre-expanding the hole with an oversize mandrel (Reference 3). This latter process, commonly known as coldworking, differs from interference fit applications mainly in that the hole is allowed to radially unload prior to inserting the fastener. This unloading results in a large compressive stress field next to the edge of the hole which improves fatigue life. Coldworking precracked fastener holes has been shown, for example, to increase the cyclic life by two orders of magnitude in some cases (Reference 4).

In order to analytically predict the service life of coldworked holes, it is necessary to examine the residual stress field caused by the pre-expansion process. An early study of the plastic deformation of holes in flat rings and disks is discussed in Chapter 33 of Reference 5. Although the applications discussed in that report center about the practice of interference fitting small tubes into industrial boilers and condensors, their form of solutions for stresses in the plastic region are employed here for the coldworked fastener hole problem. Several authors have examined the stress fields around interference fit fasteners by both experimental (References 2, 6-7) and analytical or numerical procedures (References 8-10). However, analysis of unloading which characterizes the coldworking process (References 11, 12) has received less attention in the published literature. The problem formulation and mathematical analysis, which provide a basis for the results presented here, are reported in References 13 and 16.

The major content in this report is in two sections, Elastic-Plastic Analysis and Discussion of Results. In the Elastic-Plastic Analysis section, deformation theory, radial symmetry and plane stress assumptions are used to model the coldworking process. Comprehensive results for finite ring geometries and arbitrary material properties are presented in graphical form. In the Discussion of Results section, the features of the graphs which seem most significant from a designer's viewpoint are emphasized. The graphs indicate that the region of yielding during pre-expansion characterizes the residual hoop stresses which presumably inhibit crack growth. A relation between this region of yielding and the mandrel interference leads to an analytical optimum interference. A comparison between analytical optimums and experimentally determined mandrel interferences which produce maximum fatigue life shows very good agreement. Thus, it is suggested that the cause of the beneficial effects of coldworking is correctly characterized and the analytical optimum interference corresponds to the mandrel interference that leads to maximum fatigue life. The major ideas are included in the summary.

SECTION II

ELASTIC-PLASTIC ANALYSIS

1. MATHEMATICAL MODEL

The geometry for which the coldworking process is modeled is depicted schematically in Figure 1. We consider a hole of radius a in a circular sheet of elastic-perfectly plastic material with outer radius b. The coldworking process involves radially expanding the hole with a mandrel to produce yielding (loading), then removing the mandrel (unloading). The region where yielding occurs during expansion is determined by a loading elastic-plastic boundary, ρ, and the region where yielding occurs during unloading is determined by an unloading elastic-plastic boundary, ρ'. Assumptions of plane stress and radial symmetry are employed in modeling the process. Deformation theory is used to relate plastic strains to total stress and the Von-Mises yield criterion is used to define the constant yield surface for plastic flow. The continuum equations are averaged through the thickness of the plate.

For the loading process, the equations consistent with these assumptions are (Reference 13).

$$\frac{du}{dr} = \frac{1}{E'}\,(\sigma_r - \nu'\sigma_\theta) + \frac{1}{3}\lambda(2\sigma_r - \sigma_\theta) \tag{1}$$

$$u/r = \frac{1}{E'}\,(\sigma_\theta - \nu'\sigma_r) + \frac{1}{3}\lambda(2\sigma_\theta - \sigma_r) \tag{2}$$

$$\frac{d\sigma_r}{dr} = \frac{1}{r}(\sigma_\theta - \sigma_r) \tag{3}$$

$$\lambda \geq 0 \text{ when } \sigma_o^2 = \sigma_r^2 + \sigma_\theta^2 - \sigma_r\sigma_\theta$$

$$\lambda = 0 \text{ when } \sigma_o^2 > \sigma_r^2 + \sigma_\theta^2 - \sigma_r\sigma_\theta \tag{4}$$

where the variables u, σ_r, σ_θ, and λ depend on r, the distance from the center of the hole, and represent, respectively, the averaged radial displacement after the loading, the radial and circumferential components of stress after loading, and the proportionality factor associated with plastic flow during loading. Note that du/dr and u/r are the radial and circumferential strains -- the first terms on the right-hand side of Equations 1 and 2 represent elastic strains and the second terms, plastic strains. The material constants E' and ν' are respectively the modified Young's modulus and modified Poisson's ratio (Reference 14) given by

$$E' = \frac{E(1+2\nu)}{2(1+\nu)} \quad \text{and} \quad \nu' = \frac{\nu}{1+\nu}$$

where E and ν are the usual Young's modulus and Poisson's ratio. The material constant σ_o is the yield stress determined from the uniaxial stress/strain curve and is equal to the effective stress for perfectly plastic modeling (Reference 15).

For the unloading process, the constitutive relations (Equations 1 and 2) are modified to include the permanent deformations due to loading according to Reference 16.

$$\frac{dw}{dr} = \frac{1}{E'}(t_r - \nu' t_\theta) + \frac{1}{3}\lambda'(2t_r - t_\theta) + \frac{1}{3}\lambda(2\sigma_r - \sigma_\theta) \tag{5}$$

$$w/r = \frac{1}{E'}(t_\theta - \nu' t_r) + \frac{1}{3}\lambda'(2t_\theta - t_r) + \frac{1}{3}\lambda(2\sigma_\theta - \sigma_r) \tag{6}$$

where w, t_r, t_θ, and λ', represent respectively, the averaged residual radial displacement field, averaged radial and circumferential components of residual stress, and proportionality constant associated with plastic flow during unloading. Observe that the residual strains $\frac{dw}{dr}$ and $\frac{w}{r}$ are comprised of elastic strains due to locked in residual stresses and

permanent deformations resulting from plastic flow during loading and unloading. The residual stresses and unloading plastic proportionality factor satisfy Equations 3 and 4 with σ_r, σ_θ, and λ replaced by t_r, t_θ, and λ'.

It is not transparent, but it has been shown in References 13, 16 that the relations in Equations 1-6 uniquely determine u, σ_r, σ_θ, λ, w, t_r, t_θ, and λ' when four consistent boundary conditions are given. For the loading process, the physical boundary conditions are the mandrel interference, u_o, and the free surface at the outer radius, i.e.,

$$u(a) = u_o \qquad \sigma_r(b) = 0$$

characterizes loading. Both inner and outer surfaces are free in the unloading process; thus

$$t_r(a) = 0 \qquad t_r(b) = 0$$

characterizes unloading.

It should be emphasized that because of radial symmetry, deformation theory as applied above leads to the same results as the Prandtl-Reuss flow theory (Reference 15). The Prandtl-Reuss theory is the basis for the finite element analysis implemented by various researchers (References 8, 10, 11, 12) investigating plane stress problems similar to the cold-working problem. Thus, the analysis herein is a semi-exact solution to compare with finite element analyses except that some of the finite elements analyses include the effect of strain hardening. A strain hardening model, e.g., a Ramberg-Osgood representation of the uniaxial stress/strain curve, could be added to the relations (Equations 1-4) at a moderate expense in the computational effort required to solve the equations.

2. METHOD OF SOLUTION

Given geometry, b/a, and material constant, E, ν, σ_o, a solution to the nonstandard two point boundary value problems which model the cold-working process is uniquely determined by specifying u_o. However, it is shown in Reference 13 that u_o must satisfy $0 \leq u_o \leq u_o^*$, where u_o^* is a maximum radial displacement for which the equations have a solution. The parameter u_o^* is interesting as a candidate for an optimum interference level and is discussed later. The field quantities in the loading process are implicitly determined by the loading elastic-plastic boundary -- the implicit algebraic relations are presented in the appendix. Hence, there is an algebraic relation between u_o and ρ. It is shown in Reference 13 that this relation is one-to-one for u_o which satisfy $u_o^e \leq u_o \leq u_o^*$ where u_o^e is that mandrel interference that just produces yielding.

The procedure used to solve the two point boundary value problem was to determine ρ from u_o using a Newton-Raphson scheme. With ρ determined, σ_r, σ_θ, and u are expressed analytically. It turns out that the unloading elastic-plastic boundary ρ' can be expressed analytically in terms of ρ. Then the residual fields t_r, t_θ, and w can be obtained from implicit analytical expressions in ρ and ρ' except that the unloading plastic flow proportionality factor, λ', must be determined by numerical integration. Thus that portion of residual displacement field where plastic flow occurs during unloading is the only field quantity that is computed numerically, and this numerical computation is quite amenable to accuracy checks. Computations for a complete solution require less than a second of CDC 6600 central processor time; thus parameter studies are quite inexpensive.

3. PARAMETRIC SOLUTIONS

Mathematically, there are four situations that can occur depending on the size of the mandrel interference. They are:

a. purely elastic loading and unloading

b. plastic flow during loading only

c. plastic flow during loading and unloading

d. no solution

The interesting situations for modeling the coldworking process are b and c which occur when u_o is in the interval (u_o^e, u_o^*). In order to concisely summarize results, the following normalizations are introduced for stress and displacement fields

$$\tilde{\sigma} = \frac{\sigma}{\sigma_o} \qquad \tilde{u} = \frac{uE'\sqrt{3}}{a\sigma_o}$$

and the distances r, ρ, and ρ' are given in terms of hole radii. It turns out that all dimensionless curves depend on b/a and ν but are universal for material properties E and σ_o.

General results for the elastic-plastic equations are presented in Figures 2-8. Poisson's ratio was fixed at $\nu = 0.3$. The u_o, ρ relationship is presented in Figure 2 for values of b/a ranging from b/a = 3 to b/a = 40. As discussed in the appendix, the maximum value of $\tilde{\rho}$ varies from $\tilde{\rho} = 2.96$ for b/a = 2.96 to $\tilde{\rho} = 1.75$ for infinite b/a. These curves are universal for the elastic-plastic problem except for a small dependence on ν which will be discussed later.

Stress and displacement fields for mandrel in and mandrel out situations are presented in Figures 3-6. Dimensionless mandrel interference is varied over the range $(\tilde{u}_o^e, \tilde{u}_o^*)$ and b/a is fixed at 40 (essentially an infinite outer radius). In Figure 3, the corners in the hoop stress curves occur at the loading elastic-plastic boundary, ρ. The additional corner

in the residual hoop stress curves occur at ρ' (Figure 5). The effects of finite geometry on stress and displacement fields are illustrated in Figure 7 -- the parameter b/a is varied over the same range as in Figure 2. The dimensionless interference is fixed at 7 corresponding to a situation where, according to Figure 2, geometry affects ρ. The relationship between mandrel interference, loading elastic-plastic boundary, and residual deformation at the hole, w_o, is presented in Figure 8. These data are limited to a single geometry, b/a = 40. An interpretation of the data displayed in Figures 2-8 is presented in the next section.

Poisson's ratio has little influence on the dimensionless solutions for even moderate coldworking levels; hence no curves are presented to illustrate its effect. Poisson's ratio enters the problem through the elastic strains; so a quantitative feel for the influence of Poisson's ratio is obtained by taking the ratio of elastic to total strains at the hole.

SECTION III

DISCUSSION OF RESULTS

1. SIGNIFICANCE OF PRESENT RESULTS

It is generally agreed that the increase in fatigue life observed for coldworked holes is attributable to the residual compressive hoop stresses at the hole. The residual hoop stresses tend to counteract the tensile stress concentrations which would otherwise occur in remote loading situations. Figures 3 and 5 indicate that the loading elastic-plastic boundary is a good measure of the size of the region where there are compressive residual hoop stresses. It is striking how the region of compressive stresses is enhanced by unloading. This suggests that interference fit fasteners might be effective even when loosely fitting if they were initially torqued sufficiently to produce substantial yielding at the hole. At any rate, ρ is a possible measure of the effectiveness of a given mandrel interference in suppressing growth of radial cracks; hence, the curves in Figure 2 relating ρ and u_o may be quite useful to the designer in visualizing the coldworking effects for different mandrel interferences.

In particular, there is a maximum value, ρ_m, for the loading elastic-plastic boundary which corresponds to u_o^*, the maximum allowable mandrel interference (Figure 2). Since u_o^* leads to the maximum region of residual compressive stresses, it's reasonable to interpret u_o^* as a mathematical optimum interference level. From a tolerance standpoint, it's interesting to note that the maximum ρ is almost obtained for a broad range of mandrel interferences preceding u_o^*. Experimentally determined optimum interference levels are compared with u_o^* in a later section.

In view of the minor influence of Poisson's ratio on solutions, the data presented in Figures 2-8 is comprehensive for this modeling of the coldworking process in the sense that the effects of material properties and ring geometry are displayed. The major effects of material properties enter algebraicly through the normalizations. In particular, the dimensionless parameter $\frac{E'\sqrt{3}}{\sigma_o}$ characterizes the primary effect of material properties, e.g., for a fixed geometry, the optimum percent interference u_o^*/a scales with $\frac{\sigma_o}{E'\sqrt{3}}$:

$$u_o^*/a = \tilde{u}_o^* \frac{\sigma_o}{E'\sqrt{3}}$$

The major effect of b/a is in determining the largest ring of yielding which can be produced by coldworking. Hence, the optimum radial expansion, $\tilde{u}_o^*$, is affected by geometry (Figure 2). Figure 7 indicates that, for fixed u_o, the effect of b/a on residual stress field near the hole is insignificant, and both Figures 2 and 7 indicate that infinite geometry is a good approximation for b/a > 10.

The u_o and ρ vs w_o curves in Figure 8 are presented to show the possibility of determining the amount of coldworking (as indicated by ρ or u_o) by simply measuring the hole diameter before and after the coldworking process. The actual mandrel interference may not be easy to measure if the mandrel deforms as well as the material around the hole. At least one manufacturer (Reference 17) has specified the coldworking process in terms of initial and residual hole diameters.

2. OPTIMUM INTERFERENCE LEVELS

In order to maximize the fatigue life improvement due to the coldworking process, the designer needs to select the proper amount of radial expansion u_o. In current practice the optimum interference level

is usually based on a series of fatigue tests (References 3,4). Since the optimum expansion would be expected to vary with material and hole diameter, this empirical approach can be both excessively expensive and time consuming for use in design.

As suggested earlier, the beneficial effects of coldworking may be characterized by the loading elastic-plastic boundary ρ, since ρ determines the size of the residual stress fields. In particular, there is a maximum ρ and corresponding maximum u_o. This maximum mandrel interference, u_o^*, may be considered an optimum level since it leads to the largest region of compressive hoop stresses.

For convenience, a graphical representation between $\frac{u_o^* E' \sqrt{3}}{\sigma_o}$ and hole radius a is given in Figure 9 for the large plate case (b/a=10). Poisson's ratio was specified as 0.3, but as discussed, varying ν for other practical values has a relatively small effect on the results. Thus, from Figure 9, one may specify the material properties E' and σ_o, select a hole radius, and readily determine the radial expansion u_o required to cause the maximum elastic-plastic boundary ρ.

In order to test the hypothesis that u_o^* is the optimum expansion from a fatigue life standpoint, experimental data reported in References 3 and 19 is included in Figure 9. The data of Reference 3 were obtained from a series of constant amplitude fatigue tests on coldworked holes in which the amount of mandrel interference was the variable. The specimens contained initially unflawed holes which were drilled, reamed, and coldworked in a manner consistent with common manufacturing practice. The holes in the 2024-T851 aluminum specimens were unfilled and loaded remotely, while the 7075-T6 aluminum members were subjected to partial load transfer through a fastener placed in the hole as would occur in an actual structure. As the interference level was increased, the

constant amplitude fatigue life (cycles to failure) tended to approach a maximum value. However, the increase in fatigue life gradually levels off as the interference is increased, thus, it was sometimes difficult to precisely locate the optimum interference within the experimental scatter. The minimum expansion required for this maximum fatigue life was selected as the optimum interference for that hole size. The data point on Figure 9 from Reference 19 is the result of a similar set of experiments with interference fit fasteners in which constant amplitude fatigue life was also measured as a function of fastener interference.

As seen in Figure 7 the experimental data generally agree quite well with the hypothesis that u_0^* represents an optimum value of radial expansion for fatigue life. In addition, the gradual approach to the experimental optimum is consistent with the flattening of the ρ vs u_0 curve, Figure 2, and suggests that there may be a desirable large tolerance in specifying the mandrel interference. In this regard, note from Figure 5 that there is little difference in residual hoop stresses for 6.9 and 8.3 dimensionless interferences and 8.3% is near optimal. A key point here is that Figure 2 gives the designer a feel for near optimal as well as optimal interferences. In fact, physical limitations of actual manufacturing equipment may preclude reaching the theoretical maximum expansion values in some cases. The mandrels used to coldwork the steel specimens sometimes failed, for example, at the loads required to pull the mandrel at the larger interference levels (Reference 3). Thus, both the relations between ρ and u_0 shown in Figure 2 and the optimum theoretical values shown in Figure 9 should be quite useful to the designer, since they provide a fatigue life criteria for selecting an interference level for a new material and hole size.

SECTION IV

CONCLUSIONS

The deformation theory of plasticity has been used to determine the residual stress and displacement fields caused by pre-expanding a hole in a circular disk with an oversize mandrel. Since fatigue rated mechanical fastening systems commonly employ interference fit or pre-expansion to develop a beneficial residual stress field about the fastener, this problem has considerable engineering interest. The results obtained here are presented in a general form which should assist in predicting the performance of many specific fastener applications. In addition, by explicitly using radial symmetry, the approach is inherently more accurate and economical than finite element techniques. The method could be extended to include strain hardening effects.

In Figure 3, the hoop and radial stress distributions caused by various interference fits are presented in a dimensionless form which allows determination of the stress distribution by simply inputting the appropriate material properties and interference conditions. These "mandrel in" curves model the behavior for interference fit type fasteners. The residual stresses occurring after the hole is allowed to radially unload are given in a similiar general form in Figure 5. These "mandrel out" curves represent the coldworking process which is receiving increased interest for use in fatigue critical areas. Comparing Figures 3 and 5, one notices that the radial unloading allows a much larger compressive residual hoop stress to be developed next to the edge of the hole than the corresponding "mandrel in" configuration.

An analytical optimum radial expansion u_0^* is proposed which would allow the engineer to maximize the fatigue improvement in the coldworking process. The analysis developed here indicates that there is a

maximum loading elastic-plastic boundary ρ_m developed by the radial expansion which is dependent only on geometric factors. The proposed optimum interference level u_o^* is the radial expansion which causes ρ_{max}. For convenience, $\frac{u_o^* E' \sqrt{3}}{\sigma_o}$ is plotted versus hole size in Figure 9. As shown, experimental data taken from the literature for three materials agree quite well with the hypothesis that u_o^* is the optimum radial expansion from a fatigue life standpoint. Thus, the curve of Figure 9 should allow the designer to maximize the fatigue improvement resulting from the cold-working process.

REFERENCES

1. R. J. Gran, et al., Investigation and Analysis Development of Early Life Aircraft Structural Failures, Technical Report AFFDL-TR-70-149, Wright-Patterson Air Force Base, Ohio, March 1971.

2. J. A. Regalbuto and O. E. Wheeler, "Stress Distribution from Interference Fits and Uniaxial Tension," Experimental Mechanics, Vol. 10, No. 7, pp 274-280, July 1970.

3. J. L. Phillips, Sleeve Coldworking Fastener Holes, Technical Report AFML-TR-74-10, Wright-Patterson Air Force Base, Ohio, February 1974.

4. G. J. Petrak and R. P. Stewart, "Retardation of Cracks Emanating from Fastener Holes," Engineering Fracture Mechanics, Vol. 6, No.2, September 1974, pp 275-282.

5. A. Nadai, Theory of Flow and Fracture of Solids, McGraw-Hill, New York, 1950, Chapter 33.

6. H. T. Jessop, C. Snell, and G. S. Holister, "Photoelastic Investigation on Plates with Single Interference-Fit Pins with Load Applied to Plate Only," The Aeronautical Quarterly, Vol. 7, November 1956, pp 297-314.

7. H. T. Jessop, C. Snell, and G. S. Holister, " Photoelastic Investigation on Plates with Single Interference-Fit Pins with Load Applied (a) to Pin Only, and (b) to Pin and Plate Simultaneously," The Aeronautical Quarterly, Vol. 9, May 1958, pp 147-163.

8. M. Allen and J. A. Ellis, Stress and Strain Distribution in the Vicinity of Interference Fit Fasteners, Technical Report AFFDL-TR-72-153, Wright-Patterson Air Force Base, Ohio, January 1973.

9. J. H. Crews Jr., "An Elastic Analysis of Stresses in a Uniaxially Loaded Sheet Containing an Interference-Fit Bolt," NASA Technical Note NASA-TN-D-6955, Langley Research Center, Hampton, Virginia, October 1972.

10. J. H. Crews Jr., "An Elastoplastic Analysis of a Uniaxially Loaded Sheet with an Interference-Fit Bolt," NASA Technical Note NASA-TN-D-7748, Langley Research Center, Hampton, Virginia, October 1974.

REFERENCES (CONTINUED)

11. W. F. Adler and D. M. Dupree, Stress Analysis of Coldworked Fastener Holes, Technical Report AFML-TR-74-44, Wright-Patterson AFB, Ohio, March 1974.

12. D. F. Green and J. P. Gallagher, "Allowable Stresses for Cracked Coldworked Holes," Technical Memorandum AFFDL-TM-74-165-FBE, Wright-Patterson AFB, Ohio, August 1974.

13. T. W. Ting and R. M. Potter, "The Problem of Forced Fittings," Archives of Rational Mechanics and Analysis, Vol. 58, No. 1, 1975, pp 77-94.

14. A. E. H. Love, A Treatise on the Mathematical Theory of Elasticity, 4th Ed., Dover, New York, 1944.

15. A. Mendelson, Plasticity: Theory and Application. Macmillan Co., New York, 1968.

16. T. W. Ting and R. M. Potter, "Problem of Forced Fittings, Part II. The Unloading Process," Internal Report, Applied Mathematics Lab., ARL, Wright-Patterson AFB, Ohio, September 1973.

17. Technical Literature on Seamless Sleeve Coldworking Method. J. O King, Inc., Atlanta, Georgia 30318.

18. R. M. Richard and J. R. Blakelock, "Finite Element Analysis of Inelastic Structures," AIAA Journal, Vol. 7. No. 3, March 1969.

19. J. H. Crews, Jr., "Analytical and Experimental Investigation of Fatigue in a Sheet Specimen with an Interference-Fit Bolt," NASA Technical Note NASA-TN-D-7926, Langley Research Center, Hampton, Virginia, July 1975.

APPENDIX

1. ANALYTICAL EXPRESSIONS FOR FIELDS

Results in References 5, 13, 16 can be used to obtain analytical expressions for stress and displacement fields after loading and residual stress field after unloading. Stress fields after loading are given by

$$\sigma_r(r) = \begin{cases} \frac{2\sigma_o}{\sqrt{3}} \sin(\phi(r)-\pi/6) & a \le r \le \rho \\ \sigma_o[1+3(b/\rho)^4]^{-\frac{1}{2}} [1-(b/\rho)^2] & \rho \le r \le b \end{cases}$$

$$\sigma_\theta(r) = \begin{cases} \frac{2\sigma_o}{\sqrt{3}} \sin(\phi(r)+\pi/6) & a \le r \le \rho \\ \sigma_o[1+3(b/\rho)^4]^{-\frac{1}{2}} [1+(b/\rho)^2] & \rho \le r \le b \end{cases}$$

where ϕ is related to r by

$$\frac{\sqrt{3}\, b^2 e^{-\sqrt{3}\phi_\rho} \sin(\phi_\rho)}{r^2} = \exp(-\sqrt{3}\phi(r)) \cos(\phi(r)) \qquad (A.1)$$

and ϕ_ρ is related to ρ through

$$\sin^2(\phi_\rho) = 1/[1+3(b/\rho)^4] \qquad (A.2)$$

The corresponding radial displacement field after loading is given by

$$u(r) = \begin{cases} \frac{r}{2E'} [(1-2\nu')\sigma_r(r) + (2\sigma_\theta(\rho)-\sigma_r(\rho)) \exp[\sqrt{3}(\phi_\rho-\phi(r))] & a \le r \le \rho \\ \frac{r}{2E'} [\sigma_\theta(r)-\nu'\sigma_r(r)] & \rho \le r \le b \end{cases}$$

The residual stress field is given by

$$t_r(r) = \begin{cases} \frac{2\sigma_o}{\sqrt{3}} \sin(\psi(r)-\pi/6) & a \le r \le \rho' \\ \frac{t_r(\rho')-\sigma_r(\rho')}{1-(b/\rho')^2}\left[1-(b/r)^2\right]+\sigma_r(r) & \rho \le r \le b \end{cases}$$

$$t_\theta(r) = \begin{cases} \frac{2\sigma_o}{\sqrt{3}} \sin(\psi(r)+\pi/6) & a \le r \le \rho' \\ \frac{t_r(\rho')-\sigma_r(\rho')}{1-(b/\rho')^2}\left[1+(b/r)^2\right]+\sigma_\theta(r) & \rho' \le r \le b \end{cases}$$

where ψ and r are related by

$$\frac{-a^2\sqrt{3}\exp\frac{-\pi 7\sqrt{3}}{6}}{2r^2} = \exp(-\psi(r)\sqrt{3}\cos(\psi(r)) \qquad (A.3)$$

and ρ' is determined from Equations A.1, A.2, A.3, and

$$\frac{b^2\sqrt{3}}{\rho'^2}\left[\sin(\psi(\rho')) - \sin(\phi(\rho'))\right] = \left[\cos(\psi(\rho')) - \cos(\phi(\rho'))\right]$$

The residual displacement field is given by

$$w(r) = \begin{cases} \frac{r}{E'}\{t_\theta(r)-\sigma_\theta(r)-\nu'(t_r(r)-\sigma_r(r')+\lambda'(r)(2t_\theta(r)-t_r(r)\}+u(r) & a \le r \le \rho' \\ \frac{r}{E'}\left[t_\theta(r)-\sigma_\theta(r)-\nu'(t_r(r)-\sigma_r(r)\right]+u(r) & \rho' \le r \le b \end{cases}$$

where $\lambda'(r)$ satisfies the ordinary differential equation

$$\frac{d\lambda'}{dr} = -[(2\lambda'+3/E')\frac{d}{dr}(t_\theta+t_r)-\frac{3}{E'}\frac{d}{dr}(\sigma_\theta+\sigma_r)]/(2t_\theta-t_r)$$

subject to $\lambda'(\rho') = 0$.

2. EXTREME VALUES FOR ρ_{max}

The maximum loading elastic-plastic boundary occurs when $\sigma_r(a) = \frac{-2\sigma_o}{\sqrt{3}}$ (the maximum stress consistent with the Von-Mises yield criterion). The relation between ϕ and r for this situation is

$$\frac{a^2 \exp\left(\frac{\pi\sqrt{3}}{3}\right)}{2r^2} = \exp\left(-\phi(r)\sqrt{3}\cos\left(\phi(r)\right)\right) \qquad (A.4)$$

Case 1 (Infinite geometry): From Equation A.2, infinite b implies $\phi_\rho = 0$; then Equation A.4 yields

$$(\rho_{max}/a) = [\exp(\pi\sqrt{3}/3)/2]^{1/2} \approx 1.75$$

which is the smallest possible value of ρ_{max}/a.

Case 2 (Completely plastic ring): It can be shown that the largest ρ_{max} obtains when the ring is completely plastic, i.e., where $\rho_{max} = b$.

The largest ratio of b/a that sustains a completely plastic ring is given in Reference 5 as

$$(b/a)^2_{max} = \exp\left(\frac{\pi\sqrt{3}}{2}\right)/\sqrt{3};$$

thus the largest value of ρ_{max} is given by

$$(\rho_{max}/a) = \left(\exp\left(\frac{\pi\sqrt{3}}{2}\right)/\sqrt{3} \right)^{1/2} \approx 2.963$$

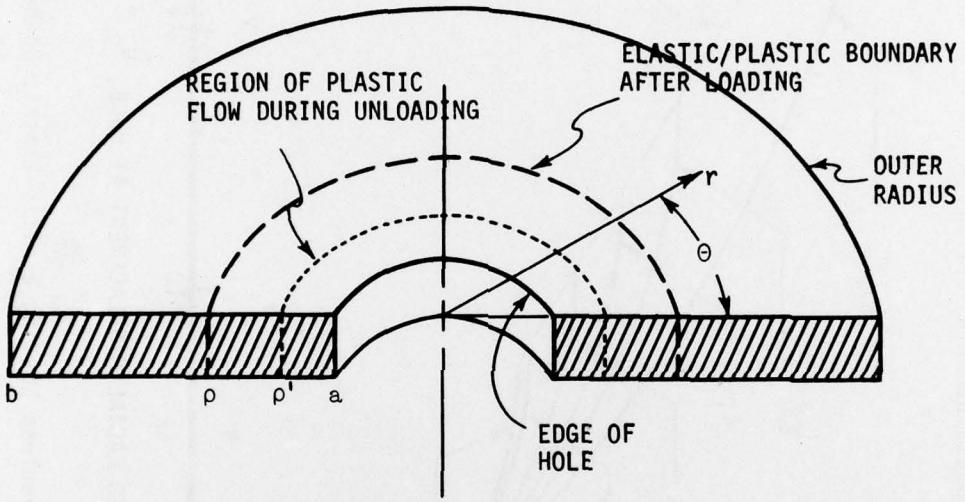

Figure 1. Geometry of Coldworking Process

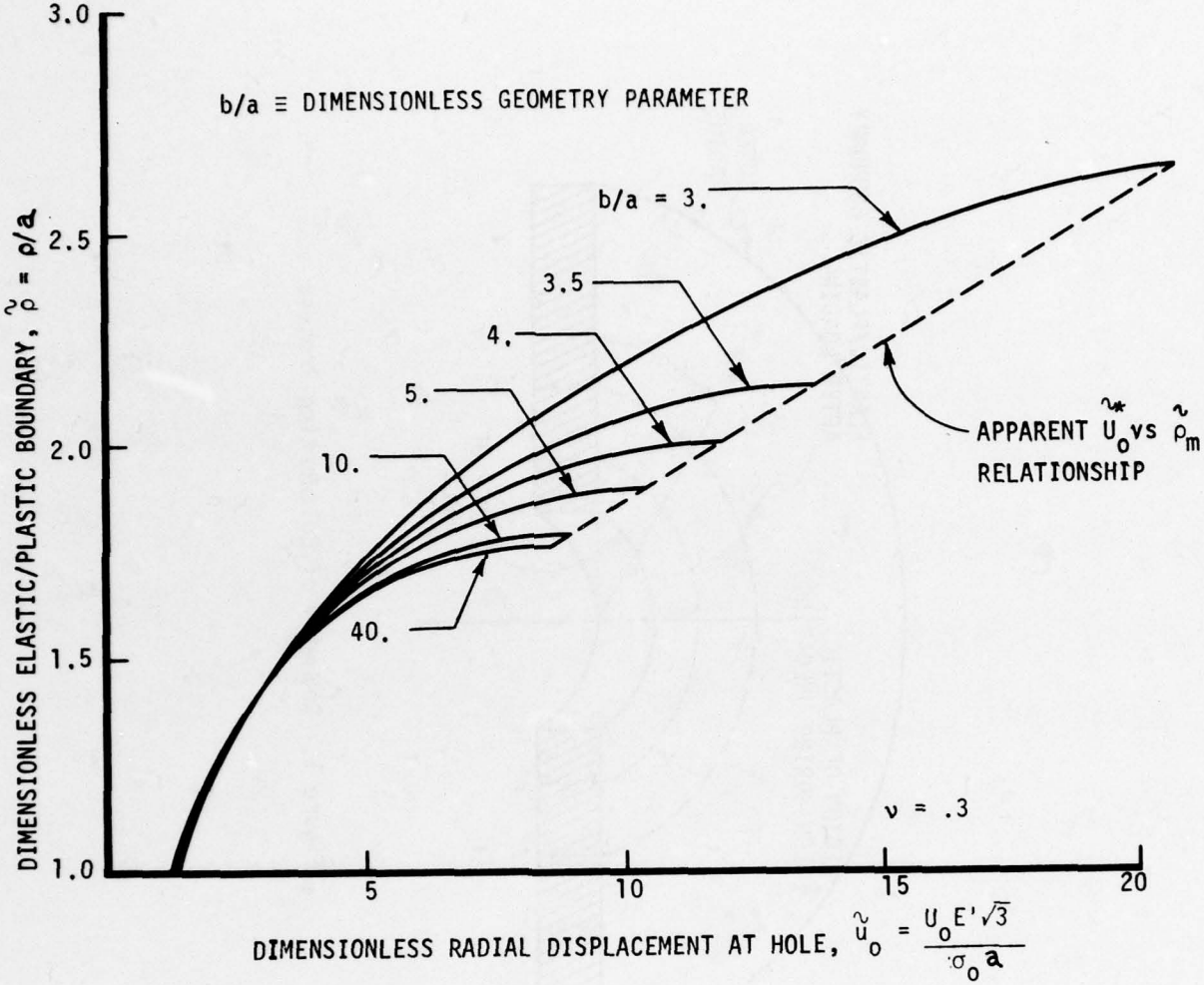

Figure 2. Dimensionless Loading Elastic-Plastic Boundary, $\tilde{\rho}_m$, vs Dimensionless Radial Displacement at the Hole, $\tilde{\mu}_o$

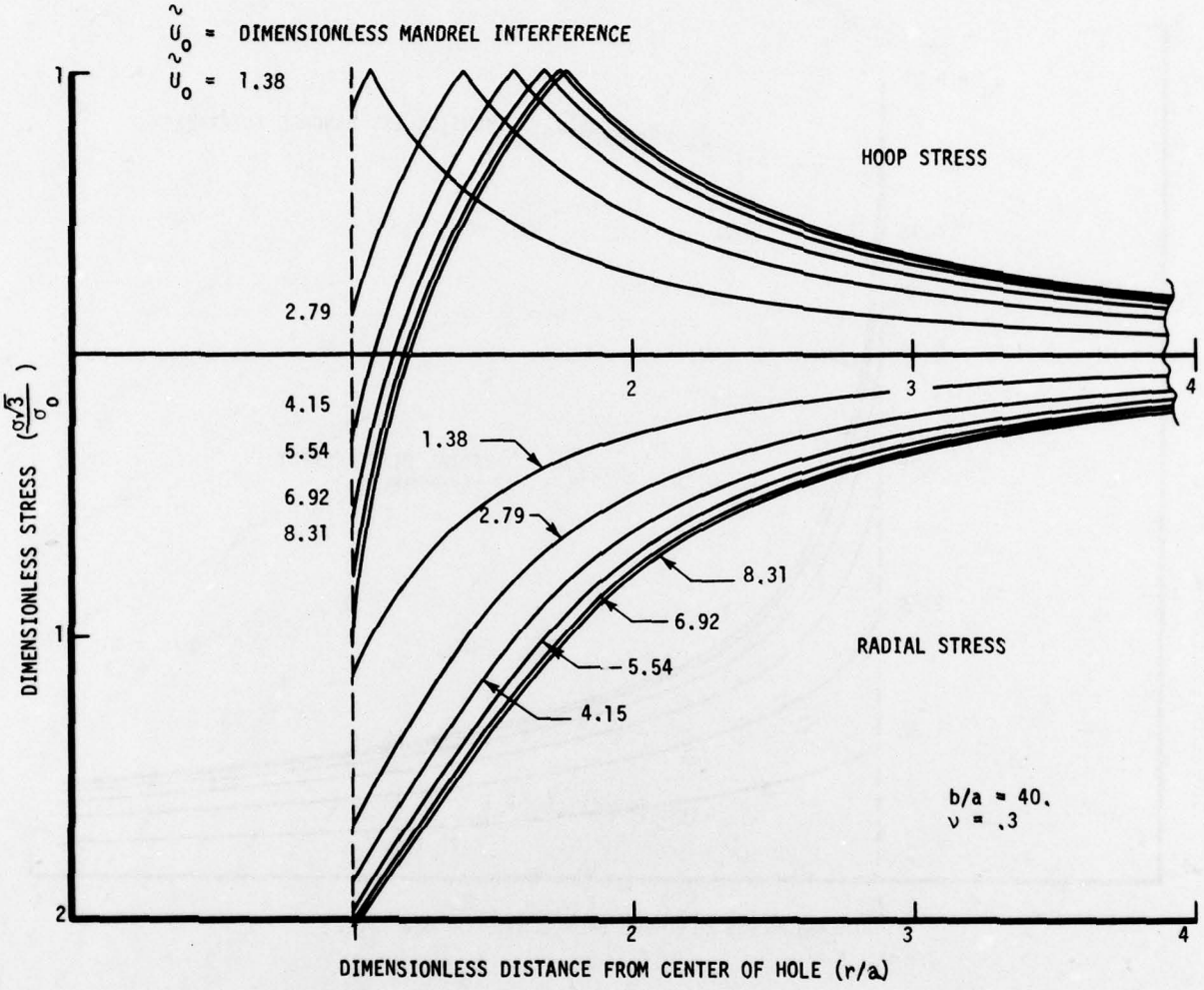

Figure 3. Dimensionless Hoop & Radial Stress, σ/σ_o vs r/a, After Loading - Mandrel In

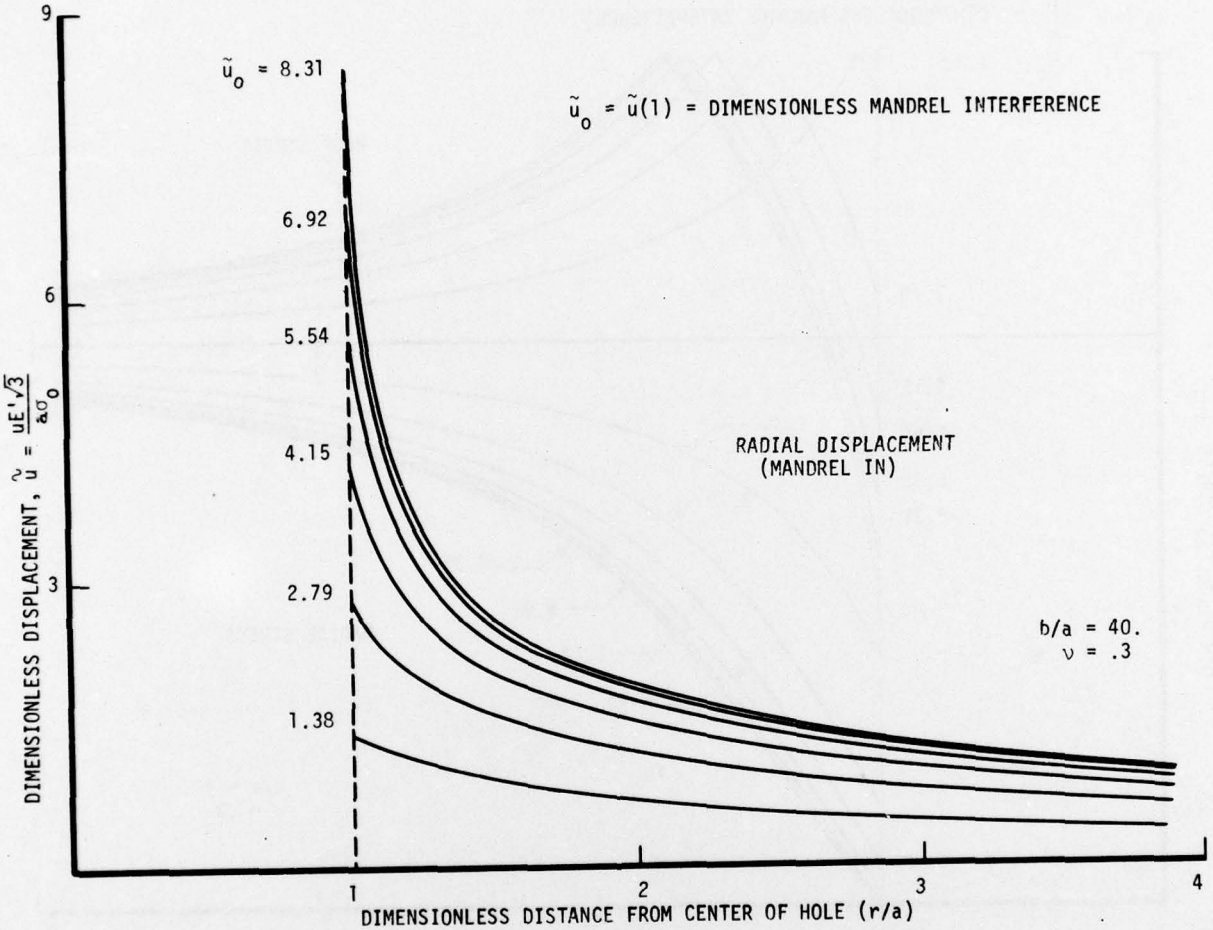

Figure 4. Dimensionless Radial Displacement Field ($\tilde{u}$ vs r/a) After Loading

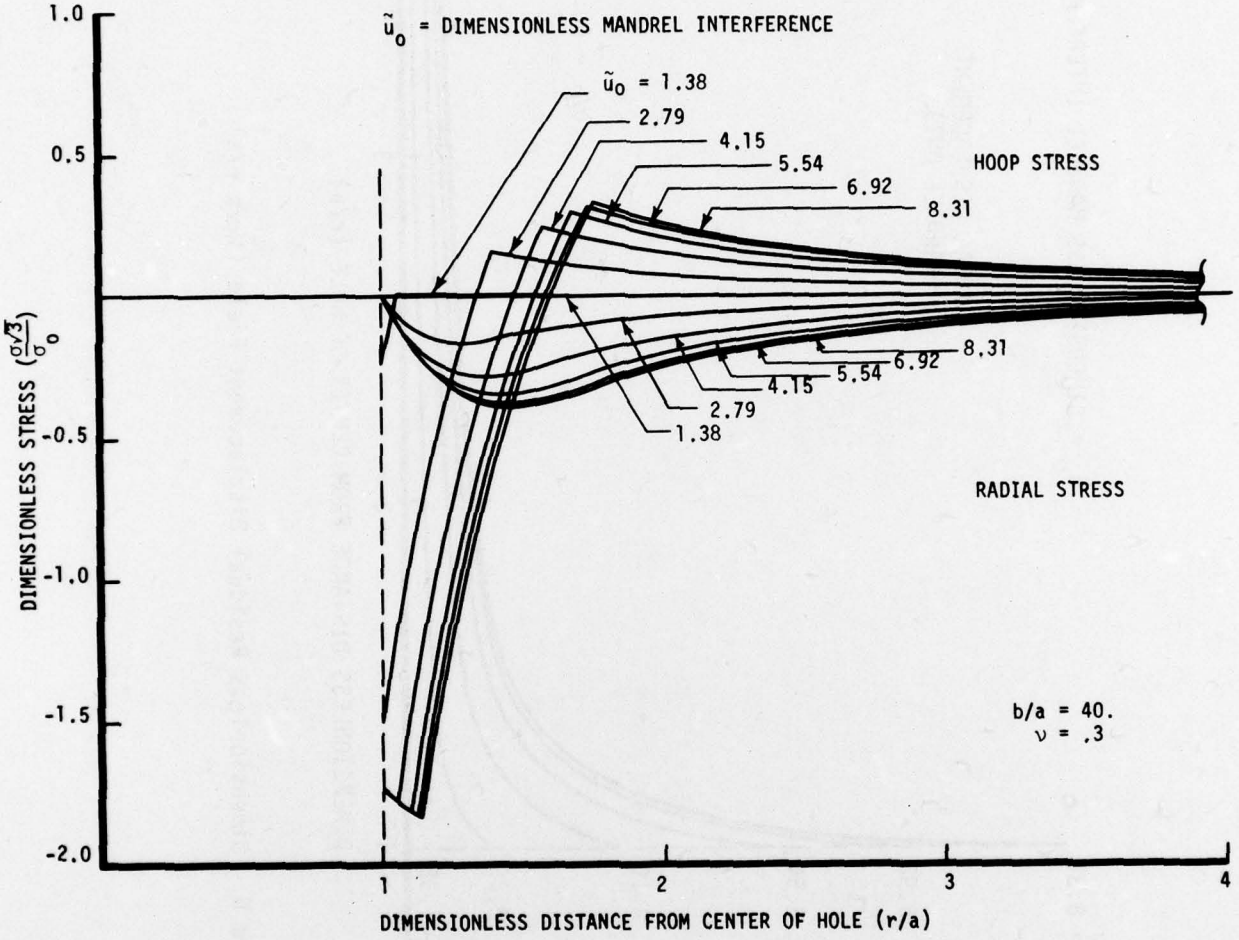

Figure 5. Dimensionless Radial Stress After Unloading - Mandrel Out

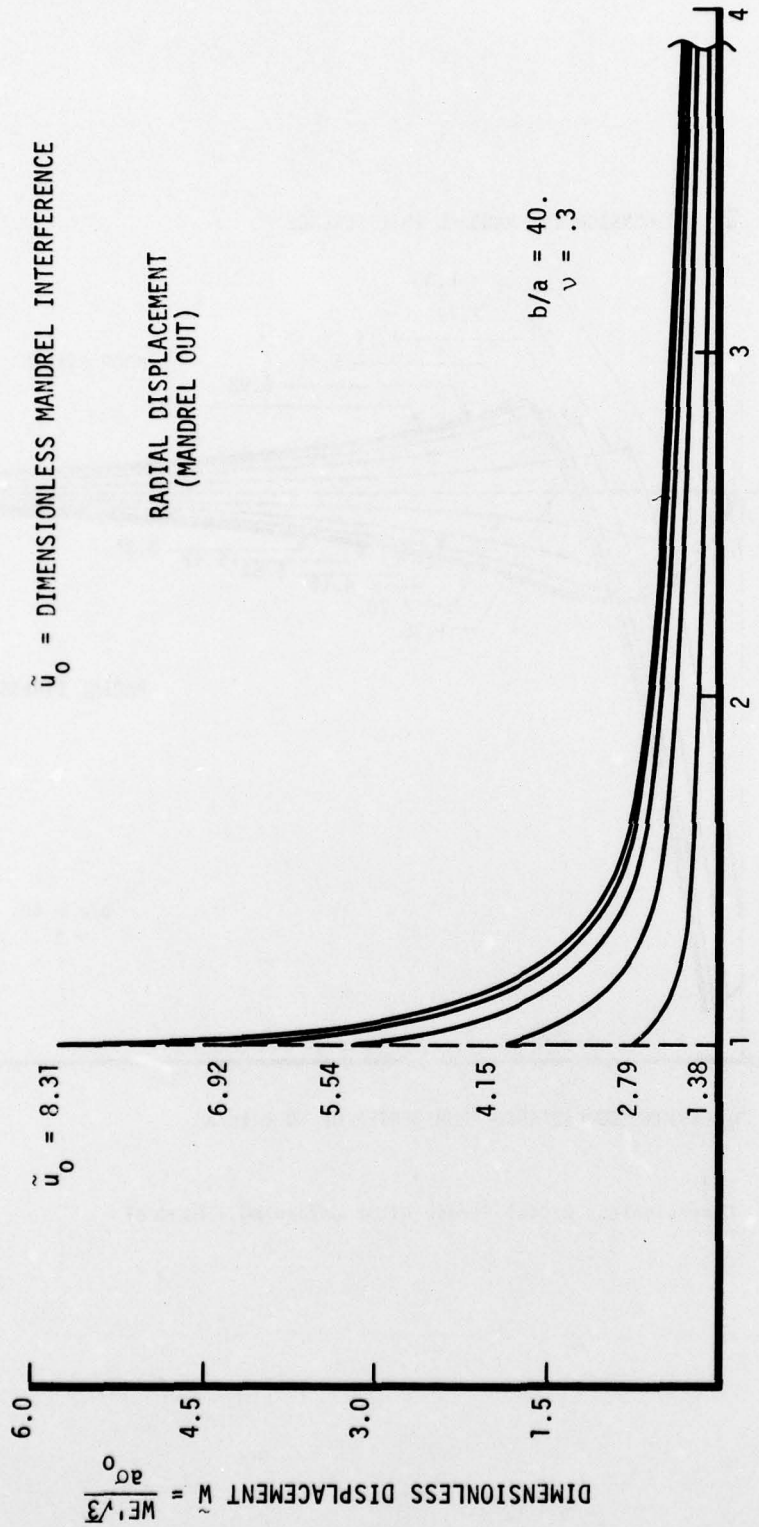

Figure 6. Dimensionless Residual Displacement Field ($\tilde{W}$ vs r/a)

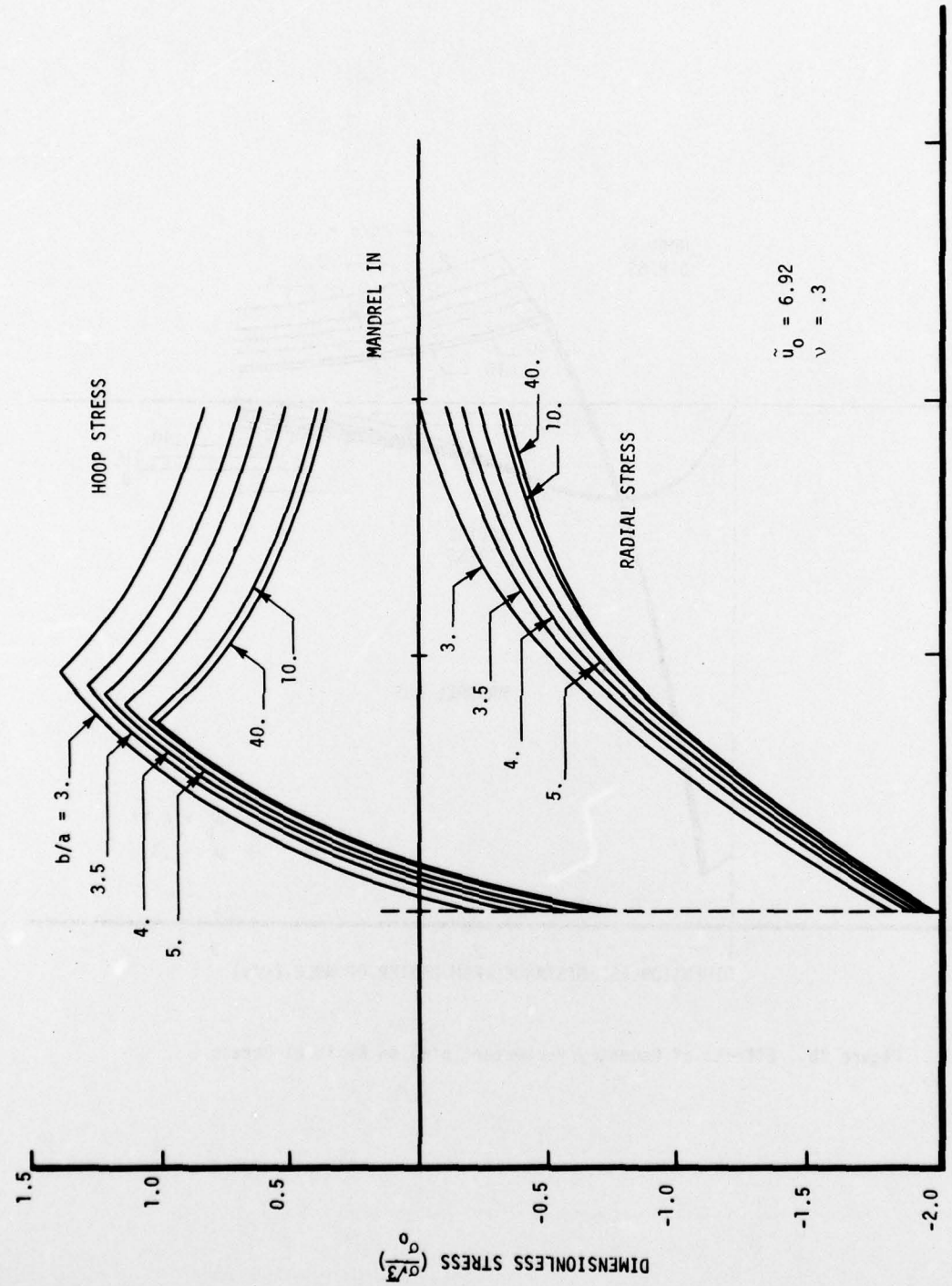

Figure 7a. Effects of Geometry Parameter (b/a) on Stress After Loading

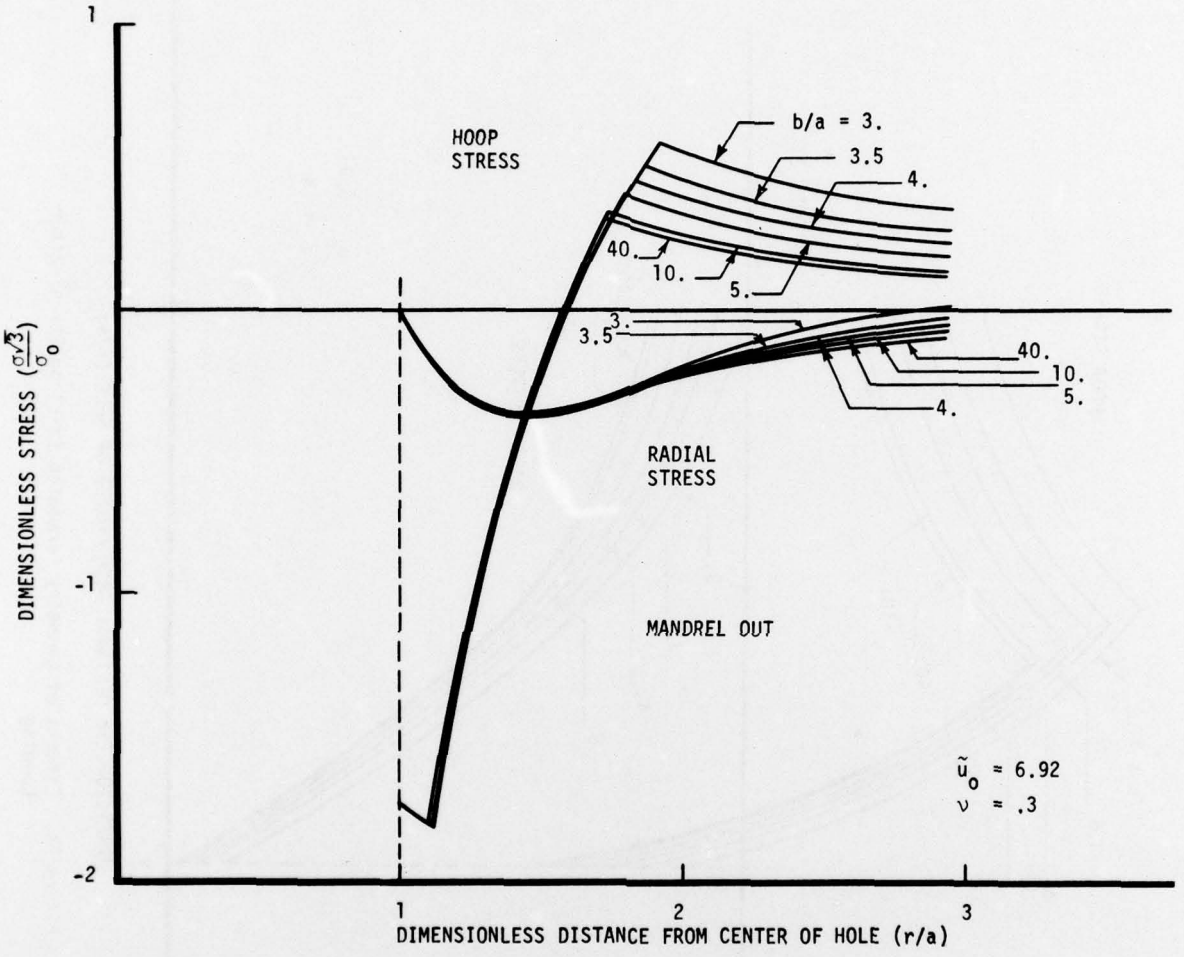

Figure 7b. Effects of Geometry Parameter (b/a) on Residual Stress

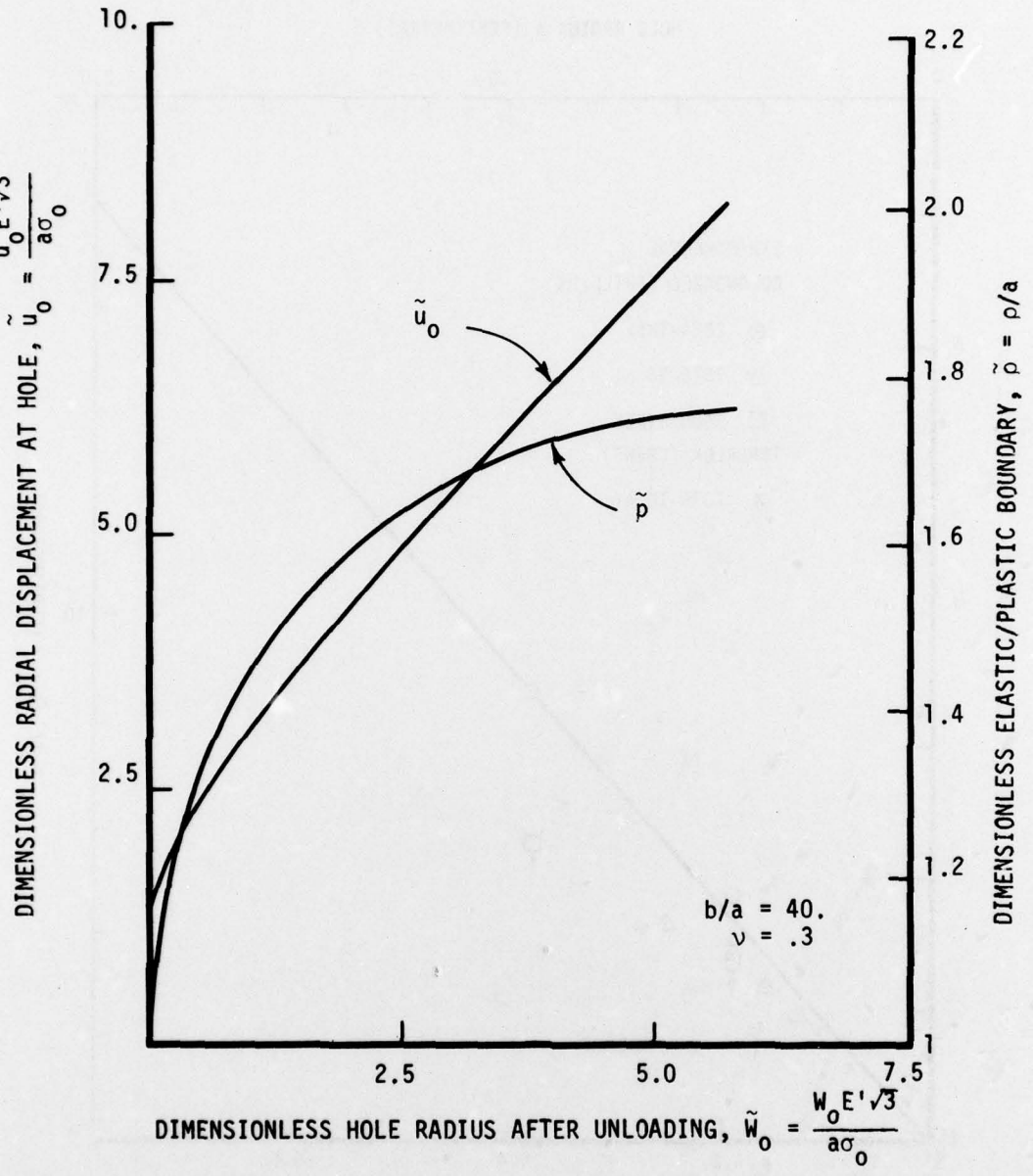

Figure 8. Dimensionless Radial Displacement, $\tilde{u}_o$, and Elastic-Plastic Boundary, $\tilde{\rho}$, vs Dimensionless Hole After Unloading, $\tilde{W}_o$

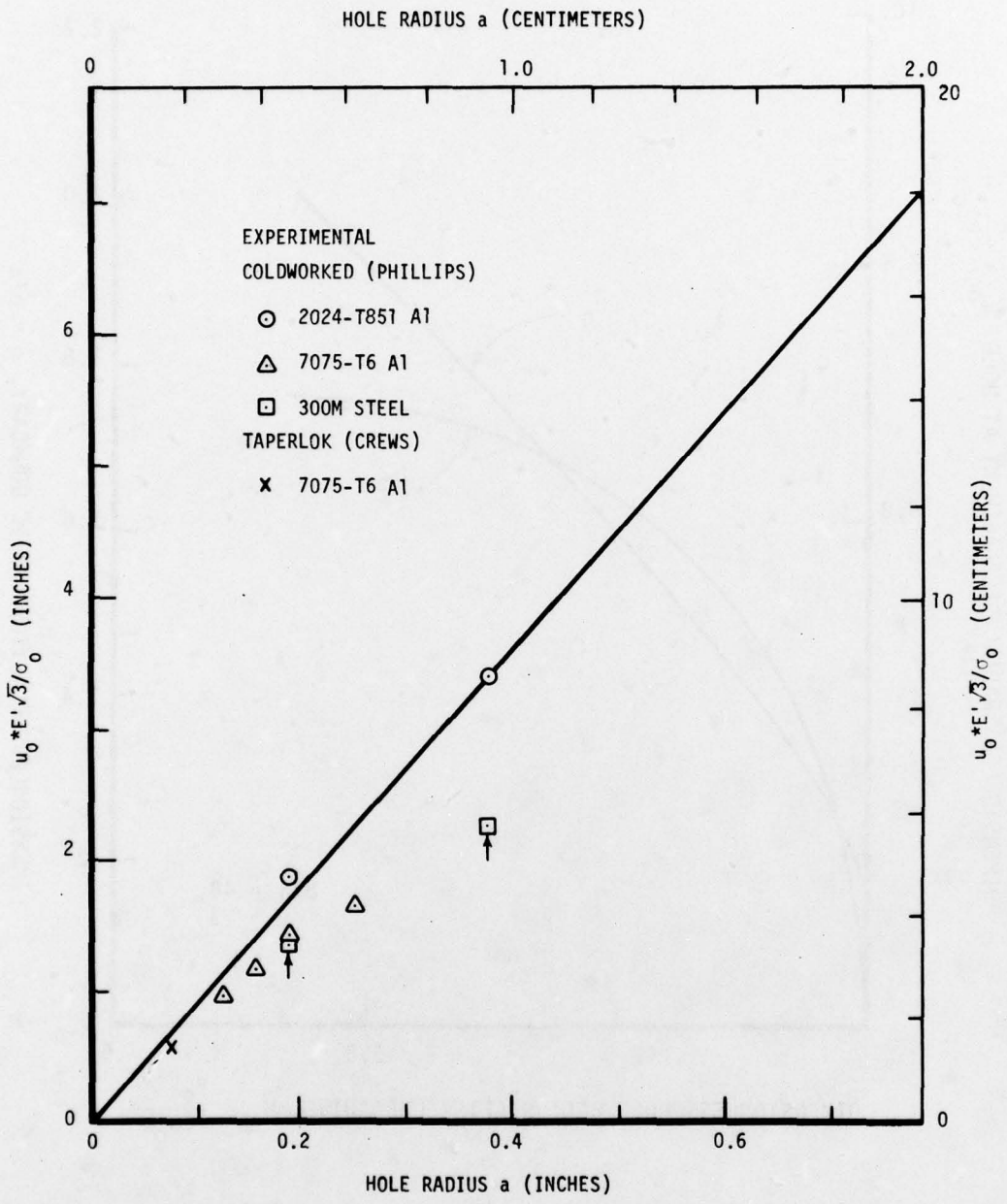

Figure 9. Comparison of Theoretical and Experimental Values for Optimum Interference Level as a Function of Hole Size

☆U.S.Government Printing Office: 1979 — 657-002/140